

Fast Gain Calibration of Photomultiplier and Electronics

Alexander Menshikov, Matthias Kleifges, Hartmut Gemmeke, Member, IEEE

Abstract—We report on a fast method for calibration of the gain of photomultiplier tubes and associated electronics. The gain was determined by the analysis of fluctuations of the signal in a fast ADC at constant illumination of photomultipliers. The theoretical description includes the effects of analogue filters, and photomultiplier afterpulses, digitization of the signal, and digital integration. In a comparison with measurements, possible errors in the calibration induced by drifts are analyzed and discussed.

I. INTRODUCTION

The presented method of statistical fluctuation analysis, as a tool for gain determination, was developed in the framework of the Pierre Auger Experiment [1]. The Pierre Auger Fluorescence Detector (FD) is designed to observe fluorescence light induced by cosmic ray extensive air showers passing through the atmosphere during dark nights. It consists of 24 telescopes, at 4 different locations, for the three-dimensional reconstruction of shower tracks. Each telescope optic focuses the light with a 14 m² mirror from a 30°x30° sky region onto a camera made of 440 photomultiplier tubes (PMT), arranged in a matrix of 20x22 pixels, see Fig. 1.

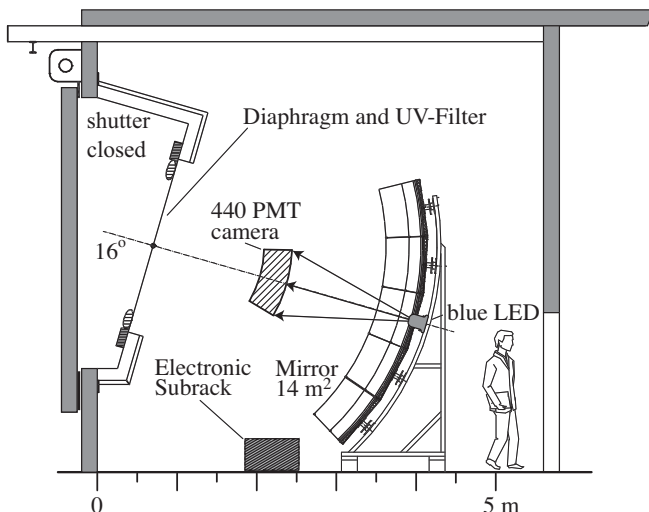


Fig. 1. The Auger Fluorescence Detector setup together with the geometry for light calibration with LED. Instead of illuminating the camera with LED light also light from a Xe-flasher can be used.

Each PMT is powered by a positive high voltage (HV) at the anode, therefore its signal is coupled by a capacitor to a differential driver (Fig. 2). The differential signal is

transferred via twisted-pair cable to the front-end amplifier.

The front-end amplifier consists of a differential receiver, a programmable-gain amplifier (PGA) and an anti-aliasing 4th order Bessel filter [2]. The photon and photoelectron collection efficiency of the system, the gain of the PMT and associated electronics, the time constants of the filter and the AC-coupling and their changes with time have to be included in the data evaluation and response function of the detector. This is quite common to most photon detector experiments.

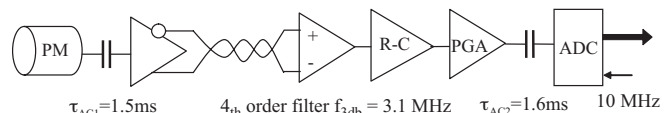


Fig. 2. A simplified scheme of the AUGER FD readout electronics from PMT to ADC including the time constants for differentiation and integration.

A precise energy scale of the FD-detector, especially its stability, is of eminent importance for the proof of ultra-high energy cosmic ray events beyond 10²⁰ eV. An absolute optical calibration by an absolute calibrated light source is normally a difficult and time-consuming procedure. To achieve a sufficient isotropy of the light source a large (diameter 2.5 m) portable half-sphere (drum) with diffuse reflector walls and UV-LEDs at the center was developed [3]. The drum calibration is good for precise measurements performed several times a year, but not appropriate for fast tests. However, a prompt calibration after interesting events is necessary several times during a night of observation.

To overcome this problem fibers distributing Xenon flasher light [4] were installed in the center of the mirror (see Fig. 1) and at several other places in the optics to allow a quick calibration. “Quick,” means here due to the limited repetition rate about 15 minutes of calibration time. The pulses of the Xenon flasher were integrated to give a relative calibration between all PMTs of one telescope. With the aid of the above-mentioned drum calibration an absolute calibration related to incoming photons instead of photoelectrons was achieved. Using the fluctuation of the digital integral of each Xe-flasher pulse the gain of the PMT, together with the electronics, could be calculated [5]. We will use for this method the name “*integral fluctuation analysis*,”.

In this work a blue LED instead of a Xe flasher is used as calibration light source. It is driven by a switched current source to generate up to 70 μs long light pulses. These pulses are long enough to yield about 600 usable ADC-samples per pulse due to the 10 MHz sample rate of the ADC. The ADC-values are written continuously to a 1000 sample long buffer (100 μs) for further use [6], [7]. Built-in

Accepted for publication in IEEE-Transaction of nuclear science 2002.

All Authors are with the Forschungszentrum Karlsruhe, 76021 Karlsruhe, Germany (corresponding author H.Gemmeke: ++49-7247-82-5635; fax: ++49-7247-82-5594; e-mail: gemmeke@ipe.fzk.de).

hardware continuously evaluates the fluctuations of the background level [8] and gives, with very high precision, the level of background fluctuations (used in this work). The variance of the signal from sample to sample together with the mean value at constant light level allows us to evaluate the gain of each PMT and electronics as described in section III. However, the filter time constants of the electronics have to be taken into account. Therefore in section II the transfer function of the analogue electronics is evaluated. Finally the method is tested with some measurements (section IV) and compared to other calibration methods mentioned above. The possible disturbance by background, photomultiplier afterpulses, and drifts of gain or light level is discussed. Because of the analysis of individually sampled amplitudes, we name this method the “amplitude fluctuation analysis,,,

II. TRANSFER FUNCTION OF THE SYSTEM

For a precise determination of the calibration the transfer function of electronics has to be considered. Several methods were used to obtain a sufficiently simple and accurate description.

A. Measurements with a spectrum analyzer

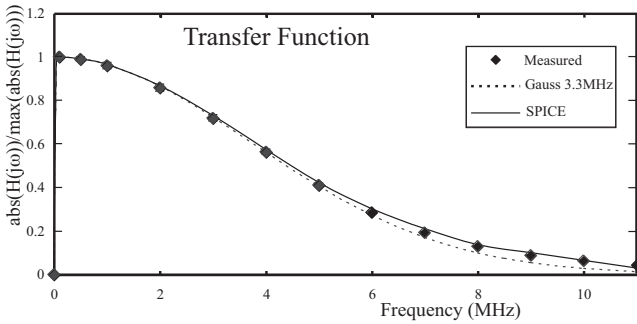


Fig. 3. Magnitude of the normalized transfer function of analogue electronics: measured values (squares), Gauss-Fit (dotted line), and SPICE-simulation (solid line).

The transfer function of the complete amplification chain including differential driver was investigated with a spectrum analyzer. All 22 channels of a front-end board were measured for middle, maximum, and minimum gain settings. The magnitude of the normalized transfer function is shown in Fig. 3. The absolute gain varies from channel to channel by not more than 2.5 %. The variation of the 3 dB cutoff frequency of the amplifier from channel to channel is also rather small, the mean value is 3.1 MHz and the deviation does not exceed 2.5 %. The low 3 dB cutoff frequency induced by the AC-coupling in the circuit (Fig. 2) is about 120 Hz corresponding to a differentiation time constant of $\tau_{AC} = 0.8\text{ms}$. This value may vary considerably from channel to channel due to 20% tolerances of the used large ceramic capacitors.

B. SPICE-Simulation

The amplifier was investigated with a SPICE simulation as well. The calculated transfer function of the amplifier is also shown in Fig. 3. The cutoff frequency 3.15 MHz obtained from the simulation is slightly larger than the measured one. The SPICE simulation was also used to analyze the sensitivity of the transfer function to tolerances

of passive components in the amplifier. We found that a 1 % tolerance in resistors and a 5 % tolerance in capacitors are sufficient to keep the deviation of the cutoff frequency below 2.5 %

C. Model of the system

The PMT together with electronics may be considered as a three stage linear system. The first stage is an amplification stage with infinite bandwidth and gain g (V/A), the second stage is an AC-coupling network characterized by a time constant τ_{AC} , and the third stage is a low-pass filter. The low-pass filter of the model has a unit gain at low frequencies. In this case the impulse response function $v(t)$ (1/s) of this filter is normalized ($\int v(t) dt = 1$).

An ideal Gaussian low-pass filter provides a quite good description of the system behavior at high frequencies. Its transfer function $H(j\omega)$ and impulse response $v(t)$ are given by the formulas:

$$H(j\omega) = \frac{1}{\sqrt{2\pi}} \exp\left(-\frac{(j\omega \cdot \tau)^2}{2}\right) \quad (1)$$

$$v(t) = \frac{1}{\tau \cdot \sqrt{2\pi}} \exp\left(-\frac{(t/\tau)^2}{2}\right) \quad (2)$$

where $\tau = \sqrt{\ln 2} / (2\pi \cdot f_{3dB})$ is related to the 3 dB cutoff frequency f_{3dB} . The normalized transfer function for a Gaussian filter with a 3.1 MHz cutoff frequency is shown in Fig. 3 as dotted line. For error analysis we also need the normalized auto-correlation function $r(\theta)$ of the impulse response, which is given by

$$r(\theta) = \frac{\int_{-\infty}^{\infty} v(t) \cdot v(t + \theta) dt}{\int_{-\infty}^{\infty} v(t) \cdot v(t) dt} \quad (3)$$

and the noise equivalent bandwidth F of the filter

$$F = \frac{1}{2} \int_{-\infty}^{\infty} |H(j\omega)|^2 d\omega = \frac{1}{2} \int_{-\infty}^{\infty} v^2(t) dt \quad (4)$$

The integrals in (3) and (4) can be calculated analytically for the Gaussian low-pass filter of (1). The autocorrelation function of the filter has also Gaussian shape

$$r(\theta) = \exp\left(-(\theta/2\tau)^2\right) \quad (5)$$

The relation between the 3 dB cutoff frequency and noise equivalent bandwidth is given by

$$F = 1 / (4\sqrt{\pi} \cdot \tau) = \frac{1}{2} \sqrt{\frac{\pi}{\ln 2}} \cdot f_{3dB} \quad (6)$$

For the Gaussian approximation we got a noise equivalent bandwidth F of 3.3 MHz.

For the measured transfer function in Fig. 3 we calculated the noise equivalent bandwidth of the low-pass filter:

$$F = \frac{1}{2} \int_{-\infty}^{+\infty} |H(j\omega)|^2 d\omega \approx \frac{1}{A_{\max}^2} \int_0^{\infty} A^2(f) df \quad (7)$$

where $A(f)$ is the magnitude of the measured frequency response of the system and A_{\max} its maximum. The normalization of the measured frequency response to its maximum value decreases the possible errors due to the spectrum analyzer. It is also necessary because of the AC-coupling of the electronics. The AC-cutoff in our case, at about 1 kHz, changes the integral by less than 0.1%. The

integral for the noise equivalent bandwidth (7) was evaluated numerically for 22 measured channels. We obtained an average value F of 3.3 MHz, the channel-to-channel deviation of F is smaller than 2.7 %.

III. GAIN OF PMT AND ELECTRONICS AS RESULT OF A FLUCTUATION ANALYSIS

Illumination of a PMT may be considered as bombarding the PMT photocathode with a sequence of photons described by a Poisson process [9]. The emission of photoelectrons from the photocathode is also a Poisson process.

A. A response of the system to light-pulses

In our model the spectral performance of the system is determined by the anti-aliasing filter with its impulse response function $v(t)$ (1/s) and the AC-coupling network with its time constant τ_{AC} . The composite impulse response function $v_{AC}(t)$ of the AC-coupled anti-aliasing filter is well approximated by

$$v_{AC}(t) \approx v(t) - \frac{1}{\tau_{AC}} \exp\left(-\frac{t}{\tau_{AC}}\right) \quad (8)$$

if the noise equivalent bandwidth F as defined in (4) is considerably larger than $1/\tau_{AC}$. For the following calculations we assume that the impulse response of the anti-aliasing filter is much slower than the rise and fall times of the PMT. In this case the filter determines completely the high-frequency behavior of the system. We assume that the noise of the electronics including digitization noise is small compared to the fluctuations of the photoelectron signal.

The gain g (V/A) of the system is a random value due to the statistical nature of the photoelectron multiplication and collection process in the photomultiplier. The mean value $M(g)$ of the gain is equal to the total gain G of the system. The variance $D(g)$ of the random gain is equal to the product of the squared gain of the system G^2 and the relative variance v_g of the photomultiplier [10].

B. Amplified photocurrent as a Gaussian random process

For the current of photoelectrons $i_{phel}(t)$ we can write

$$i_{phel}(t) = \sum_k e^- \cdot \delta(t - t_k), \quad (9)$$

where the random times t_k of photoelectron emission are produced by a Poisson process with the mean rate α . The Dirac function is denoted by $\delta(t)$ (1/s), and e^- (C) is the electron charge. The random signal $x(t)$ (V) at the output of our linear system is caused by the current of photoelectrons:

$$x(t) = \sum_k e^- \cdot g \cdot v_{ac}(t - t_k) \quad (10)$$

From the theory of random functions generated by a Poisson process [9] it follows that the mean $M(x(t))$ of the response of the amplifier to a step-like light impulse is well approximated by

$$M(x(t)) \approx \overline{i_{phel}} \cdot G \cdot \exp(-t/\tau_{ac}) = M_0 \cdot \exp(-t/\tau_{ac}) \quad (11)$$

and the variance of the response $D(x(t))$ is given by

$$D(x(t)) \approx \overline{i_{phel}} \cdot e^- \cdot M(g^2) \cdot \left(2F - \frac{2}{\tau_{ac}} + \frac{1}{2\tau_{ac}} \left(1 - \exp\left(\frac{-2t}{\tau_{ac}}\right) \right) \right) \quad (12)$$

$$\approx \overline{i_{phel}} \cdot e^- \cdot G^2 (1 + v_g) \cdot 2F = const := D_0$$

where the average photoelectron current $\overline{i_{phel}} = \alpha \cdot e^-$.

The approximations (11) and (12) are exact for times t considerably larger than the time constant τ of the Gaussian filter (6). For our amplifier we can neglect the dependence of the variance $D(x(t))$ on the AC-coupling constant τ_{AC} . In fact the output signal of the amplifier is the sum of a definite function equal to the mean (11) and a random function (or noise) with zero mean and variance given by (12). For relatively large illuminations, many of the individual pulses $v_{AC}(t - t_k)$ overlap with each other and the random noise distribution is well approximated by a Gaussian. The normalized correlation function of the noise is equal to the normalized auto-correlation function of the filter (5).

IV. STATISTICAL GAIN MEASUREMENTS

A. Data evaluation including correction for AC-coupling

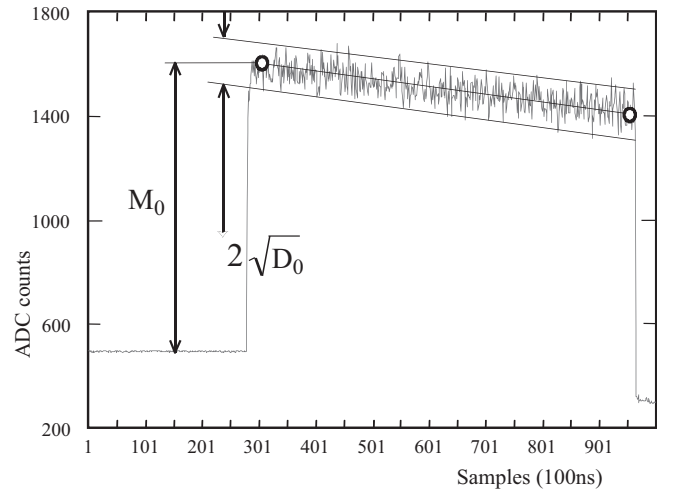


Fig. 4. A 70µs LED signal in a 100 µs frame of data taking corresponding to 1000 time slices of the fast ADC.

A series of the LED flashes provides the necessary amount of samples for evaluation of the variance D_0 and the parameter M_0 of the mean value. By the choice of the light amplitude the digitization noise was negligible against the light fluctuation. However the illumination level was kept low enough to avoid short-term gain drift of the PMTs [11]. To collect as many ADC samples as possible with a relatively few number of calibration events, we use 70 µs long LED flashes, as shown in Fig. 4. In relation to a buffer length of 1000 we select 700 to include enough baseline information. Furthermore, we only take 600 samples into account to be far off from rise and drop time effects. The slope on the top (Fig. 4) of the signal is fitted to a parabola approximating in 2nd order of the exponential drop. With this fit we get a good estimate of the parameter M_0 and the AC-coupling time constant τ_{AC} . The variance was evaluated as a mean squared deviation of the samples from the fit. We controlled the quality of this correction and the short-term stability of LED and PMTs gain, by comparison

of the amplitude at both edges of the pulse. We found very small distortions at the end of each pulse of the PMTs.

B. Distortions induced by afterpulses.

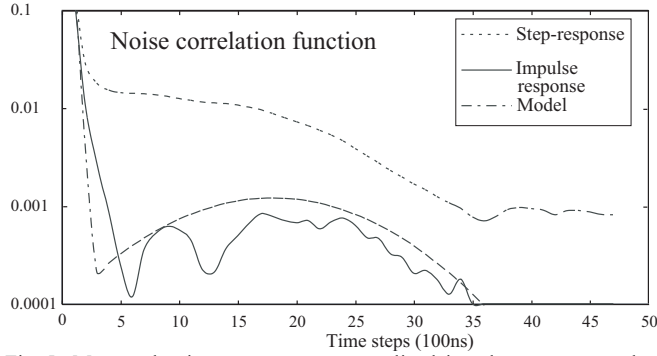


Fig. 5. Measured unit step-response, normalized impulse response and a simplified model of the noise correlation function.

One or more afterpulses may follow each photoelectron signal of the PMT. They originate from ions of the residual gases and carry charge proportional to the original signal [11]. The afterpulses are quantified by the ratio of their charge to the charge of an original photoelectron pulse and time delay distribution.

We investigated afterpulses using long LED flashes with a sharp falling edge. At first the response of each channel on the falling edge of the LED impulse was averaged over 100 LED flashes and normalized to the amplitude of the light pulse. After that an averaged response of all channels of the camera was calculated. The derivative of the step response is the normalized impulse response function of the system $v(t)$ ($\int v(t) dt = 1$). It is a sum of the responses to the original photoelectron pulse and to the afterpulses. If the afterpulses are delayed long enough by time Θ (about 500ns, see Fig.5) then they are well separated from the original pulse and yield an afterpulse ratio

$$\alpha = \frac{\int_{\Theta}^{\infty} v(t) dt}{\int_{-\infty}^{\Theta} v(t) dt} \approx \int_{\Theta}^{\infty} v(t) dt \approx 1.3\% \quad (13)$$

The accuracy of this ratio is limited by the fall time of the LED flashes, the width of the impulse response function of the amplifier and the sampling period of the ADC. Despite these restrictions we measured two well separated peaks in the delay time distribution which may be caused by different positions of ion creation in the dynode chain (short distances) or cathode area (larger drift distances). In fact the delay time distribution of the afterpulses determines the tail of the normalized impulse response, which is smoothed by the anti-aliasing filter and the sampling period.

We may consider ionization of the gaseous molecules in the PMT as a Poisson process. Therefore the afterpulses undergo in a linear system the same transformations as the photoelectron signals. The equations (11), (12) corrected by a factor $(1+\alpha)$ and $(1+\alpha^2)$ respectively give a good description of the step-function response for times larger than the afterpulses delay. As simplified model of the noise correlation function at a constant illumination we used the sum of the autocorrelation function of the filter (5) and a Gaussian fit of the delay time distribution of the afterpulses (Fig.5).

C. Integration of signal over time

The integration of the signal acts like a digital filter. The sum of N consecutive noise values gives a new random distribution. The variance depends on the number N and on the correlation of neighboring samples. The correlation is due to the anti-aliasing filter in the analog electronics and afterpulses of the photomultipliers. For Gaussian noise the variance of the sum D_{Σ} is

$$D_{\Sigma} = D_0 \cdot \left(N \cdot r_0 + 2 \sum_{i=1}^{N-1} (N-i) \cdot r_i \right) \quad (14)$$

where $r_0 = 1$, $r_i = r(i \cdot \Delta t)$ is the normalized correlation function of the noise separated by the digitization period Δt of the ADC. From the system of equations (11), (12) we eliminated the photocathode current i_{phel} and obtained an expression for the gain G measured in (V/A):

$$G = \frac{D_{\Sigma}}{M_{\Sigma} \cdot e^{-} \cdot (1 + v_g) \cdot 2F} \left(r_0 + \frac{2}{N} \sum_{i=1}^{N-1} (N-i) \cdot r_i \right)^{-1} \quad (15)$$

where $M_{\Sigma} = M_0 \cdot N$, see (11).

It is more convenient to use (ADC-counts/phel/100ns) as the unit for the gain due to our digitization interval of 100 ns. Taking into account that we measure D_0 in (ADC-counts²), M_0 in (ADC-counts) and F in (MHz) we obtain:

$$G = \frac{D_{\Sigma}}{M_{\Sigma}} \cdot \frac{10}{(1 + v_g) \cdot 2F} \cdot \left(r_0 + \frac{2}{N} \sum_{i=1}^{N-1} (N-i) \cdot r_i \right)^{-1} \quad (16)$$

Equation (16) may be simplified, if all PMT and channel specific parameters are summarized in a single calibration constant K

$$K = \frac{10}{(1 + v_g) \cdot 2F} \left(r_0 + \frac{2}{N} \sum_{i=1}^{N-1} (N-i) \cdot r_i \right)^{-1} \quad (17)$$

For the filter with cutoff frequency considerably smaller than the digitization frequency the correction coefficient doesn't depend on F and K simplifies to:

$$K \xrightarrow{N \rightarrow \infty} 1 / (1 + v_g) \quad (18)$$

That can be proven using equations (3) and (4):

$$\begin{aligned} 2F \left(r_0 + \frac{2}{N} \sum_{i=1}^{N-1} (N-i) \cdot r_i \right) &\xrightarrow{N \rightarrow \infty} 2F \cdot \sum_{-\infty}^{\infty} r_i \\ &\approx \frac{1}{\Delta t} \int_{-\infty}^{\infty} 2F \cdot r(\theta) d\theta \equiv \frac{1}{\Delta t} = 10 \text{ (MHz)} \end{aligned} \quad (19)$$

If we have no integration ($N = 1$), we get:

$$K = \frac{10}{(1 + v_g) \cdot 2F} \quad (20)$$

It seems to be not obvious to measure a gain defined as ratio of output and input amplitudes by investigating the output signal alone. But our input signal has pure random nature so that the statistical laws can be applied and we get the gain without knowing the amplitude of the input signal.

D. Amplitude versus integral method

Applying the amplitude method we get very stable gains using (16), however the result is about 10 % lower than the values determined by an integral method using the Xe-flasher [5]. In order to analyze the effect of smaller and

longer integration times we evaluate our data with different integration periods between 100 ns and 40 μ s. The results we got from three different calibration runs showed the astonishing behavior to be seen in Fig. 6.a. For short integration times we see a steep rise due to the correlation between consecutive ADC values produced by the anti-aliasing filter and afterpulses. At large integration times we had a constant rise, but of different slope from run to run. We discovered a small long-term drift of the LED amplitude. This drift causes only 0.4% gain error for the amplitude method but has an unacceptable effect for the integration method. Assuming we have a constant drift over time we get an additional term in the variance:

$$D_{\Sigma}^{\prime} = D_{\Sigma} + \text{drift}^2 / 12. \quad (21)$$

This additional term vanishes if we allow for drift amplitude correction (Fig. 6.b). The correction of the anti-aliasing filter increases the gain estimate at short integration times and the afterpulse correction lowers the gain at long integration times. Tiny short-term drifts of the PMTs gain or LED brightness may cause the rise of the gain remaining after all corrections.

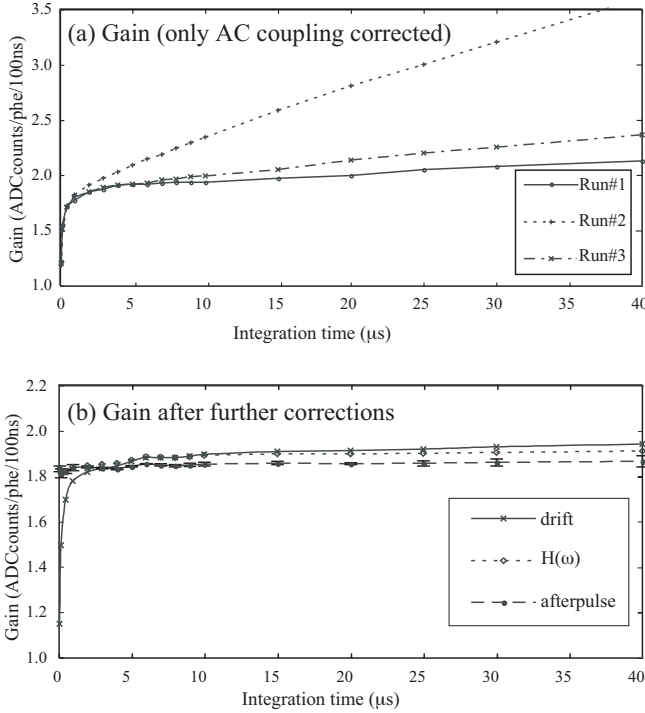


Fig. 6. Gain determination as function of integration time between 100 ns and 40 μ s corresponding to 1 to 400 time slices of a 70 μ s light pulse. The results are averaged over all pixels and 100 shots of the LED. In part (a) no corrections for drift and correlations between neighboring time slices are applied, whereas the effect of the corrections (to transfer function $H(j\omega)$, afterpulses and drifts) can be seen in part (b). For (b) it was averaged over all 3 runs.

By comparison of the gains obtained with the amplitude and integral fluctuation methods applied to the same calibration data, one can derive the individual values of the noise equivalent bandwidth F (4) for each channel of the camera. The noise equivalent bandwidth of all channels have to be evaluated only once with high statistics and low error.

E. Errors of the statistical gain measurement

The accuracy and precision of the gain measurements depends on the uncertainty of the calibration constant K and

the errors of variance and mean. D_{Σ} and M_{Σ} introduce a statistical error of the gain. The K has to be calibrated once. The parameter K contains a systematic error. The relative variance v_g of the PMT gain varies 10 % around the mean value of 0.4 if the PMTs are from the same production batch. Since the uncertainty of the noise bandwidth is below $\pm 2.7\%$ the *total systematic error of the gain will be smaller than $\pm 5.5\%$* .

The error of D_{Σ} and M_{Σ} are correlated, but together are statistically independent from the error of the calibration constant K . The upper limit of the relative gain error is given as

$$\left(\frac{\Delta G}{G}\right)^2 \leq \left(\frac{\sqrt{D(M_{\Sigma})}}{M_{\Sigma}} + \frac{\sqrt{D(D_{\Sigma})}}{D_{\Sigma}}\right)^2 + \left(\frac{\Delta K}{K}\right)^2 \quad (22)$$

Following the formulas in [12] and using the equations (14), (15) the relative random error of the gain can be expressed as:

$$\left(\frac{\Delta G}{G}\right)^2 \leq \left(\sqrt{\frac{(1+2r)D_0}{N \cdot M_0^2}} + \sqrt{\frac{2(1+r^2)D_0^2}{D_0^2}}\right)^2 / n_s + \left(\frac{\Delta K}{K}\right)^2 \quad (23)$$

where n_s is the number of statistical samples and the integration period N is the size of each sample. Each 70 μ s LED flash produces 600 ADC samples, therefore a number of flashes n_{flash} yields $600 \cdot n_{flash} / N$ statistical samples.

The M_{Σ} relative error decreases with increasing LED intensity and is negligible in comparison to the relative error of D_{Σ} already for $M_0 = 100$ (ADC-counts). The noise correlation r is as small as 0.2 and can be neglected as well:

$$\left(\frac{\Delta G}{G}\right)^2 \leq 2/n_s + \left(\frac{\Delta K}{K}\right)^2 \quad (24)$$

Our goal is to keep the additional error of the gain caused by the statistical term in (24) below 2.5%. This requires at least $3200 \cdot N / 600$ LED flashes. In the Xe-calibration the number of statistical samples is equal to the number of flashes and 3200 flashes are necessary. For the amplitude method 6 flashes are enough to reach the required accuracy.

The integral method with the Xe-flashes or with the LED pulses doesn't need the noise equivalent bandwidth F but requires many light flashes to reach high accuracy of the gain (18). The amplitude method provides the same accuracy with smaller number of light flashes but requires F for correction (20).

F. Results and comparison with other methods

Using only 100 light flashes we got 60 000 samples, sufficient (at $N = 1$) for a statistical error much smaller than the required 2.5 %. We calibrated mostly with M_0 equal 1000 ADC-counts over 600 samples within a 100 microsecond event and got a statistical error for the channels gain of 0.2 %. The used intensity of the light pulses affects the PMT gain of the camera to less than 1% [1]. Finally, we obtained a gain of 1.84 (ADC-counts/photoelectron/100ns) averaged over all 440 channels of the detector (assuming the multipliers have all the same single photoelectron resolution of $(1 + v_g) = 1.413$ as was also assumed in an analysis with the Xe-flasher [5]). Our result is consistent with calibrations

using the Xe-flasher and the drum. The amplitude and the integral fluctuation analysis applied to the drum calibration data obtained with 150 LED flashes (35 μ s long), produces the average gain of 1.74 and 1.78 (ADC-counts/photoelectron/100ns), respectively. The Xe-calibration yields calibration constants in the range of 1.88 (this work) to 2.11 (ADC-counts/photoelectron/100ns) [5] (not corrected for AC-coupling, afterpulses, and drift).

G. Equalizing the gain of the detector

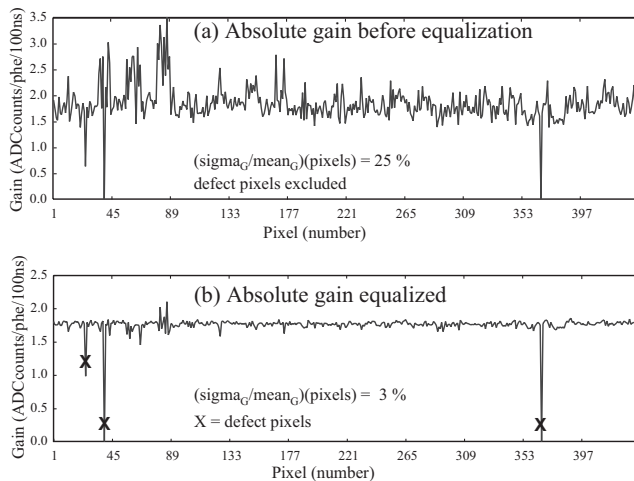


Fig. 7. Measured gains for all 440 pixels of the camera (Telescope #4 in LosLeones) in (ADC-counts/photoelectron/100 ns). In part (a) the electronic gain is preset to the same nominal value. 3 pixels are defect. The measured gain in (a) is used to obtain a more uniform gain as shown in (b).

At first the amplification of the electronics was set to the same nominal value and the absolute gain of the camera was measured by the amplitude method using 100 LED flashes, each 70 μ s long. From the measured gain we calculated amplification correction factors for each channel to obtain a uniform gain over the detector. After that the amplification of the electronics was adjusted and the absolute gain of the camera was measured again. The measured gains of all 440 PMTs of the camera before and after equalization are shown in Fig. 7. Uniformity of the camera gain is drastically improved. The channel-to-channel deviation of the gain remaining after equalization is on average 3%. In a few channels the regulation range of the PGA was exceeded and the absolute gain could not be set to the desired value.

V. CONCLUSION

The full calibration procedure for each pixel of the detector including the analysis and adjustment of the amplifiers takes a few minutes. Comparable methods using the statistics of integrated pulses (e.g. Xe-flashers [2]) need measuring times of nearly an hour to get the same precision. The described amplitude method evaluates the mean value for each macro pulse of 70 μ s and thus avoids problems due to drifts and AC-coupling. With a combination of the *integral* and *amplitude* method the noise equivalent bandwidth can be measured for each channel.

The effect of the afterpulses can be measured and corrected as well. Because of these afterpulses the amplitude method underestimates the gain approximately by a factor $(1 + \alpha) = 1.013$, whereas the integral method overestimates

the gain by the same factor. Also the crosstalk of 6×10^{-4} between the camera channels [7] does not affect the measurement results because of its very small value.

We have no indication of short-term drifts of the LED light emission during each flash. Local overheating of the LED chip and instability of the current paths in its pn-junction could possibly induce such drift. But these additional fluctuations would cause overestimation of gain values by the amplitude method in comparison to Xe-flasher, which was not observed.

VI. REFERENCES

- [1] Pierre Auger Collaboration, "Technical Design Report,, available: <http://tdpc01.fnal.gov/auger/org/tdr/index.html>
- [2] *Electronics Engineer's Handbook*, 3^d ed., D.G.Fink and D.Christiansen, Ed. , McGraw-Hill, New York, 1989, p 12-16.
- [3] J. Brack, R. Meyhandan and G.Hofman, "Prototype Auger Absolute Calibration System: Fluorescence Detector Calibration at Los Leones., GAP-2002-033. Available: http://www.auger.org/admin/cgi-bin/woda/gap_notes.pl
- [4] J.A.J.Matthews, "Optical Calibration of the Auger Fluorescence Telescopes." Proceedings of SPIE Conference on Astronomical Telescopes and Instrumentation, 22-28 August 2002, Waikoloa, Hawaii, USA
- [5] A.de Capoa, "Calibration of the FD telescope channels using light pulses., GAP-2002-005. Available: http://www.auger.org/admin/cgi-bin/woda/gap_notes.pl
- [6] H. Gemmeke, A. Grindler, H. Keim, M. Kleifges, N. Kunka, Z. Szadkowski, D. Tcherniakhovski, "Design of the Trigger System for the Auger Fluorescence Detector,," *IEEE Trans. Nucl. Sci.*, Vol 47, No. 2, April 2000, pp. 371-375.
- [7] H. Gemmeke for the Pierre Auger Collaboration, "The Auger Fluorescence Detector Electronics,," Proc. of the ICRC conference, Hamburg, 2001, on CD-ROM, ISBN 3-9804862-7-3.
- [8] M. Kleifges, A. Menshikov, D.Tcherniakhovski, H. Gemmeke, "Statistical Current Monitor for the Cosmic Ray Experiment Pierre Auger,," to be published in *IEEE Trans. Nucl. Sci.*
- [9] A.Blanc-Lapierre and R.Fortet, *Theory of Random Functions*, Vol.1, Gordon and Breach, 1968, pp 157-173
- [10] *Fast Response Photomultipliers*. Philips application book, M.D. Hull, C. Eng, Ed., Eindhoven: Philips Gloeilampenfabrieken 1971, pp 22-31
- [11] *Photomultiplier tubes, principles & applications*. S-O Flyckt, C.Marmonier, Ed., Photonis, Brive, France. 2002, pp 4_36-4_42
- [12] V.S.Pugachev, *Probability Theory and Mathematical Statistics for Engineers*, Pergamon Press, 1984, pp 227-228